

Multi-Frequency ESR Studies on Low-Dimensional Antiferromagnets, ζ-(BEDT-TTF)$_2$PF$_6$(THF) and γ-(BEDT-TTF)$_2$PF$_6$

Keisuke Maeda,*[1] Toshifumi Hara,[2] Ko Furukawa,[1,2] and Toshikazu Nakamura[1,2]

[1]The Graduate University for Advanced Studies, Myodaiji, Okazaki 444-8585

[2]Institute for Molecular Science, Myodaiji, Okazaki 444-8585

Received March 29, 2007; E-mail: kei-m@ims.ac.jp

Multi-frequency ESR measurements using X- (9.5 GHz), Q- (34 GHz), and W-band (95 GHz) microwaves, magnetic measurement using SQUID and energy band calculation were carried out on ζ-(BEDT-TTF)$_2$PF$_6$(THF) and γ-(BEDT-TTF)$_2$PF$_6$. The temperature dependence of the spin susceptibility of the two salts shows that of typical paramagnetic insulators with low-dimensional antiferromagnetic interaction. The macroscopic magnetic behaviors are apparently similar to each other, and the absolute values of the intra-chain antiferromagnetic interaction, J_{intra}/k_B, of the two salts are also close to each other. However, their ground states and microscopic behaviors indicate obvious difference. ζ-(BEDT-TTF)$_2$PF$_6$(THF) undergoes an antiferromagnetic transition at around 5 K, whereas γ-(BEDT-TTF)$_2$PF$_6$ shows no magnetic long-range ordering down to 4 K. The ESR linewidth, ΔH_{pp}, of ζ-(BEDT-TTF)$_2$PF$_6$(THF) was almost temperature independent in the paramagnetic region. On the other hand, the ΔH_{pp} of γ-(BEDT-TTF)$_2$PF$_6$ gradually decreased as the temperature was decreased. The low-temperature electronic states of these salts are discussed in the aspect of the magnetic dimensionality.

(BEDT-TTF)$_2$X salts, where BEDT-TTF is the bis(ethylenedithio)tetrathiafulvalene, have been the most extensively studied materials in the organic conductors, and are well-known to possess various ground states such as charge-order, antiferromagnetic and superconductivity phases, which occur by applying pressure or varying counter anion, X. The existence of polymorphism is also significant feature of the (BEDT-TTF)$_2$X salts. The importance of the steric terminal ethylene group has been also pointed out. Historically, the nomenclature, such as α, β, γ, ζ, and so on, has not been consistent with actual BEDT-TTF alignment. The consensus of the unified classification for various BEDT-TTF salts was given by Mori et al.[1–3] The polymorphism in (BEDT-TTF)$_2$PF$_6$ salts has been reported, and detailed research on electronic properties have been performed for the β-type PF$_6$ salt,[4,5] which has a metal–insulator transition just below the room temperature with charge disproportionation on two BEDT-TTF molecules. However, detailed electronic investigations have not been carried out for the other types of PF$_6$ salts. In this paper, we focused on two PF$_6$ salts, ζ-(BEDT-TTF)$_2$PF$_6$(THF) and γ-(BEDT-TTF)$_2$PF$_6$ (Hereafter we abbreviate them as ζ-salt and γ-salt, respectively). Although they may not be so attractive as organic conducting materials, because of recent progress in quantum spin systems and investigations on charge-localized phases, these insulating materials attract much attention at present.

For the ζ-salt, only the crystal structure has been reported. Since the donor alignment of the ζ-salt is similar to that of α'-(BEDT-TTF)$_2$AuBr$_2$,[6,7] it may be classified as an α'-phase. The ζ-salt is considered to be an insulator since the other materials attributed to α'-phase are almost insulators.[1] As for the γ-salt, the stacking mode of the BEDT-TTF is similar to that of (BEDT-TTF)$_2$FeCl$_4$,[8–10] which is classified as a δ'-phase.[1] Hence γ-(BEDT-TTF)$_2$PF$_6$ might be classified to the δ'-phase. However, it is called γ-salt in this paper following the previous report to avoid confusion. The γ-salt shows semiconducting behavior with gap varying from 60 to 80 meV in the temperature range between 290 and 140 K.

The macroscopic magnetic properties have not been reported by previous researchers. We have also performed macroscopic magnetism measurements by using SQUID as well as ESR measurements. As seen in previous X-band ESR measurements[11] for ζ-salt and γ-salt, the microscopic behaviors of the two salts are obviously different, although the macroscopic magnetic behaviors are apparently similar to each other. In order to clarify the detailed microscopic behaviors for these salts, we performed the multi-frequency ESR measurements with the results of macroscopic magnetic properties and band calculation. Multi-frequency ESR investigations are advantageous for understanding the development of spin–spin correlation and electronic dimensionality. Especially, we found the novel behavior of the ESR linewidth and g-shifts for γ-(BEDT-TTF)$_2$PF$_6$ as shown later.

In present paper, we report the results of the multi-frequency ESR measurements using X- (9.5 GHz), Q- (34 GHz), and W-band (95 GHz) microwaves and crystallographic investigation using the crystal structure analysis and energy band calculation for the γ-salt and the ζ-salt. We discuss the relationship between the dimensionality of the crystal structure and that of spin correlation.

Experimental

Crystal Preparation. Samples were prepared by an electrochemical method. BEDT-TTF (3×10^{-2} mmol) and tetrabutyl-

Published on the web January 10, 2008; doi:10.1246/bcsj.81.84

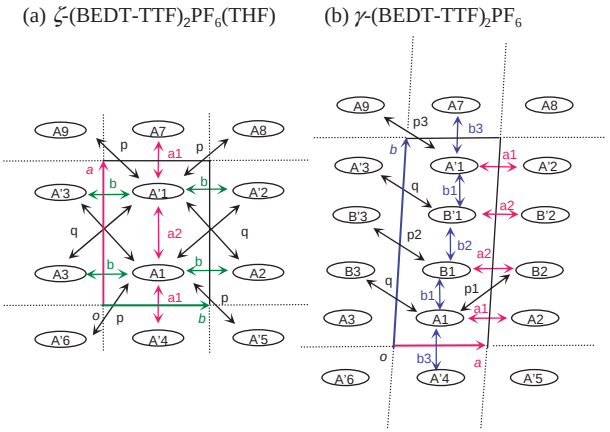

Fig. 1. Calculation model for overlap integrals. (a) ζ-(BEDT-TTF)$_2$PF$_6$(THF). (b) γ-(BEDT-TTF)$_2$PF$_6$. Molecules A and B are crystallographically independent. A–A′ and B–B′ are related by symmetry operation.

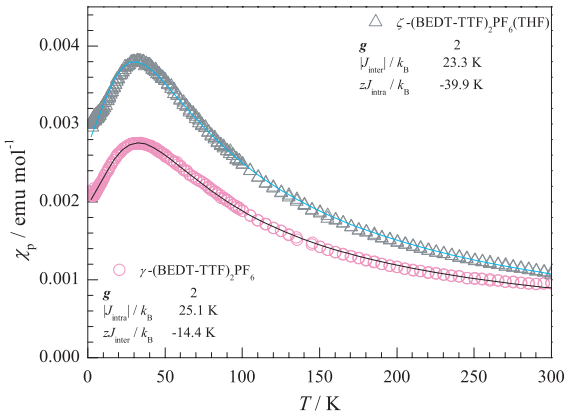

Fig. 2. Temperature dependence of the magnetic susceptibility for ζ-(BEDT-TTF)$_2$PF$_6$(THF) and γ-(BEDT-TTF)$_2$PF$_6$. The triangle and the open circle show the observed values under the magnetic field of 1 T for the ζ-salt and γ-salt, respectively. The solid curves display the calculated χ_p values based on the extended Bonner–Fisher model.

ammonium hexafluorophosphate (3×10^{-1} mmol) were dissolved in the mixed solution of 16 mL THF with 10% ethanol in H-shaped electrolysis cell. ζ-(BEDT-TTF)$_2$PF$_6$(THF) crystals were obtained as black plates on the platinum electrodes under constant current 1 μA. γ-(BEDT-TTF)$_2$PF$_6$ crystals were obtained as black needles in 16 mL of 1,1,2-trichloroethane with 10% ethanol. The crystal structure was confirmed to be consistent with the previous report[6] by the X-ray diffraction.

Static Magnetic Susceptibility Estimated by SQUID. Static magnetic susceptibility was measured by Quantum Design MPMS2 SQUID magnetometer for small single crystals about 2 mg. The sample was wrapped with plastic film and held in plastic straw. The magnetization was measured under a 1 T magnetic field in the temperature range from 2 to 300 K. The magnetic susceptibility was determined by correcting the magnetization data using Pascal's diamagnetism law.

Calculation of Overlap Integrals of Molecular Orbitals and Energy Bands. In order to support the results of ESR measurements, calculation of the conduction band energy based on a standard tight-binding approximation were performed, and the shape of Fermi surfaces were drawn. MO energy and overlap integrals were calculated using the program package developed on the basis of the extended Hückel method by Mori et al. The theoretical background is described in Ref. 12. The calculation procedures were as follows.

Molecular orbital energies were calculated for crystallographical independent molecules in the unit cell. The Slater exponents and the ionization potentials for each atom that were used were those reported in Ref. 13. The intermolecular overlap integrals S of HOMOs were calculated using the models described in Fig. 1. Only the BEDT-TTF molecules were focused in the calculations, and the counter anion was omitted in the figure, because the electric and the magnetic properties are governed by an unpaired electron on two BEDT-TTF molecules. The transfer integrals, t, were estimated by using the equation $t = ES$.

The energy bands were calculated based on the tight-binding approximation model, which is standard in the band structure study for organic conductors. Using the calculated transfer integrals and the Hamiltonians prepared based on tight-binding approximation model, the conduction bands for BEDT-TTF layers were calculated.

Multi-Frequency ESR Measurements. X- and Q-bands ESR measurements were carried out for single crystals using Bruker E500 spectrometers with rectangular resonant cavity: TE_{011} and He-flow cryostat (OXFORD ESR900). The W-band ESR spectra were measured on a Bruker E680 spectrometer equipped with He-flow cryostat (OXFORD CF935). The temperature was controlled with an OXFROD ITC503 in the temperature range from 4 to 300 K. The temperature dependence of the single-crystal ESR spectra for the ζ-salt and the γ-salt were examined under a static field, $\boldsymbol{H}_{ext}$, along the three axes, which were parallel to the principal axes of the $\boldsymbol{g}$-tensor.

Results and Discussion

Magnetic Measurements. To understand the macroscopic magnetic behavior, we performed magnetic susceptibility measurements by using a SQUID magnetometer. Figure 2 shows the temperature dependence of magnetic susceptibility, χ_p, of the ζ-salt and the γ-salt. The absolute values of the magnetic susceptibility of the ζ-salt and the γ-salt at 300 K were 1.1×10^{-3} and 0.96×10^{-3} emu mol^{-1}, respectively, which correspond to that of Curie spins of $S = 1/2$. The magnetic susceptibility of the both salts increased as the temperature decreased with a local maximum at around 34 K. It then decreased toward a finite value at 2 K. This behavior is characteristic of the low-dimensional antiferromagnetic chain. The apparent difference in the absolute value of χ_p between the two salts in the lower temperature region comes from considerable contamination of non-magnetic impurity, the β-salt, which we cannot distinguish this polymorph by the crystal shape, for the case of the γ-salt.

Hatfield et al. have reported the following two equations[14] based on the Bonner and Fisher's linear-chain theory.[15]

$$\chi_{B\text{–}H} \approx \frac{Ng2\mu_B}{k_B T} \frac{0.25 + 0.14995X + 0.30094X^2}{1.0 + 1.9862X + 0.68854X^2 + 6.0626X^3}, \quad (1)$$

where $X = |J_{intra}|/k_B T$

$$\chi_p = \frac{\chi_{B\text{–}H}}{1 - \frac{2zJ_{inter}\chi_{B\text{–}H}}{Ng^2\mu_B{}^2}}. \quad (2)$$

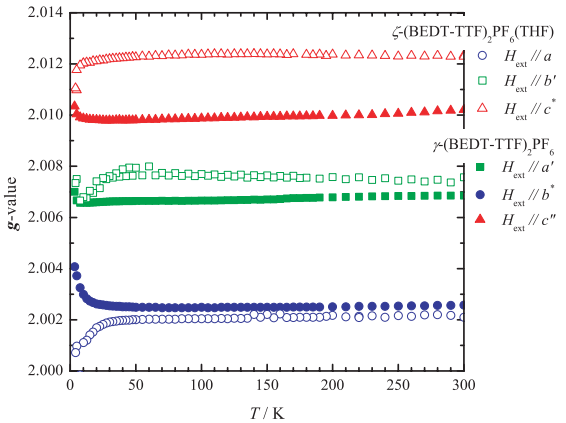

Fig. 3. Temperature dependence of g-values for ζ-(BEDT-TTF)$_2$PF$_6$(THF) and γ-(BEDT-TTF)$_2$PF$_6$ when applying the magnetic field along three principle axes.

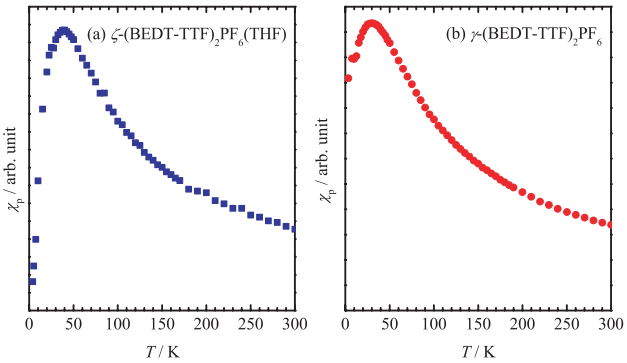

Fig. 4. Temperature dependence of spin susceptibility for ζ-(BEDT-TTF)$_2$PF$_6$(THF) and γ-(BEDT-TTF)$_2$PF$_6$ estimated from the average of the ESR signal intensity for three principle axes.

We applied this one-dimensional Heisenberg analysis involving correction for interchain interaction to the results of the magnetic measurements. An antiferromagnetic exchange interaction was estimated, although there was the ambiguity in the absolute values for the γ-salt. The evaluated intrachain and interchain interactions, $|J_{\mathrm{intra}}|/k_{\mathrm{B}}$ and $J_{\mathrm{inter}}/k_{\mathrm{B}}$ for the ζ-salt and γ-salt, are shown in the Fig. 2. The ζ-salt had considerable inter-chain interaction. Excellent fitting results indicate that the magnetic dimensionality of the ζ-salt is much larger than that of the γ-salt. To clarify the validity of this model and to understand the microscopic properties, we discuss the magnetic dimensionality from the results of ESR measurements and the electronic structure.

Multi-Frequency ESR Measurements. Multi-frequency ESR spectroscopy is a powerful method for the investigation of the spin dynamics in the various electronic states. The spin–spin correlation is reflected in the ESR linewidth. Hence, we can obtain direct information of the spin–spin correlation frequency by using Q- and W-bands besides conventional X-band ESR at various temperatures. In order to determine the microscopic magnetic properties, ESR measurements on single-crystals of the ζ-salt and γ-salt were performed. Although these two salts look like they have the same magnetic properties from the results of macroscopic magnetic susceptibility measurements, the obvious differences were found from multi-frequency ESR measurements.

The observed ESR spectra of the ζ-salt and the γ-salt were always a single Lorentzian over the entire temperature range. The number of repeating units in the cell for the ζ-salt and γ-salt is two ($Z = 2$), and these salts contain four BEDT-TTF molecules in each unit cell. For both salts, two crystallographically independent BEDT-TTF molecules appear in each unit cell. However, due to quick exchange, the ESR signal was observed as an average of two g-values.

Figure 3 shows the g-values of the ζ-salt and the γ-salt along the three principle axes as a function of temperature. At room temperature, the g-value was the largest along the molecular long axis and the smallest along the short axis. Such kind of anisotropic behavior of the g-value is easily explained by considering the principal values of the BEDT-TTF cations and their orientation.[16] The g-values were temperature independent down to around 50 K for ζ-(BEDT-TTF)$_2$PF$_6$(THF) and 20 K for γ-(BEDT-TTF)$_2$PF$_6$. Below that temperature, anomalous g-shifts were observed. For ζ-(BEDT-TTF)$_2$PF$_6$-(THF), the g-values decreased along all axes, whereas for γ-(BEDT-TTF)$_2$PF$_6$, the g-values increased.

Anomalous g-shifts are frequently observed in conventional low-dimensional antiferromagnets. Theoretical calculations on the g-shift in a one-dimensional antiferromagnet by Nagata and Tazuke[17] are well known. When an external field is applied along the direction of one-dimensional chain, the g-value shifts higher. On the other hand, when the field is applied along the normal to the chain, the g-value shifts lower. In addition, experimental results which fit to the Nagata's theory have been reported.[18] Moreover, Miyashita et al. have extended Nagata's theory and performed numerical calculations on the g-shift for various model of one-dimensional antiferromagnetic chains.[19] The effect of anisotropic interaction has been considered in their study. As a result, they have indicated that there are the systematic shifts of resonance field. However, the manner of the g-shifts for the ζ-salt and the γ-salt was quite different from that for conventional one-dimensional antiferromagnets. The g-values shifted higher for ζ-salt and lower for γ-salt when the field is applied along each direction. It might be that the anisotropic spreading of BEDT-TTF molecular orbital contributes to the anomalous g-shift. We cannot explain the experimental results at present. Further theoretical work on the g-shift is needed.

The temperature dependence of the spin susceptibility of the ζ-salt and γ-salt estimated from the integrated signal intensity of X-band ESR are shown in Figs. 4a and 4b, respectively. The spin susceptibility determined by the ESR measurement is in good agreement with that determined by SQUID magnetometer. The spin susceptibility of the two salts increased as the temperature was decreased with a local maximum at around 30 K and then decreased. The ESR signal of the ζ-salt abruptly disappeared below 5 K, indicating a magnetic long-range ordering.[20] No obvious anomaly observed at around 5 K in the magnetic measurement by SQUID probably comes from that the spin-flop field of the antiferromagnetic phase of the ζ-salt is less than 1 T. Although we performed the SQUID measurements down to 0.1 T, we could not observe a clear drop in the spin susceptibility at around 5 K, because of a poor signal to

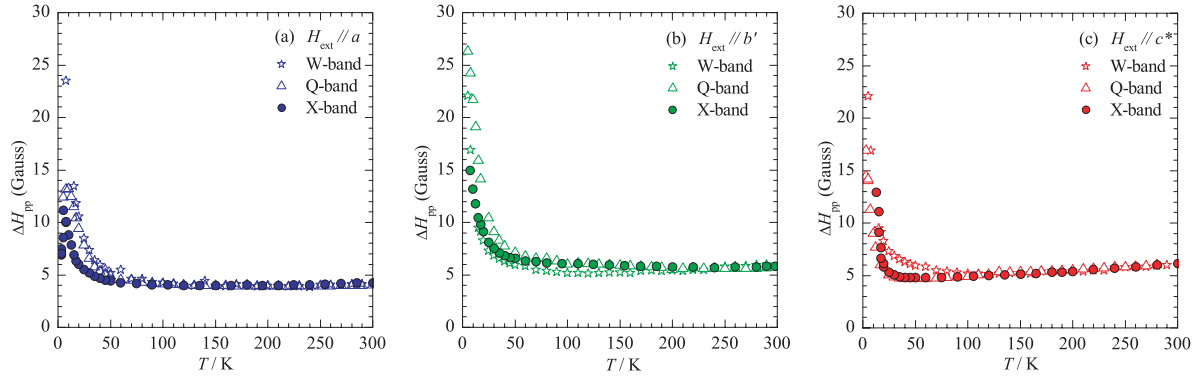

Fig. 5. Temperature dependence of ESR linewidth for ζ-(BEDT-TTF)$_2$PF$_6$(THF), applying the external magnetic field along three principle axes.

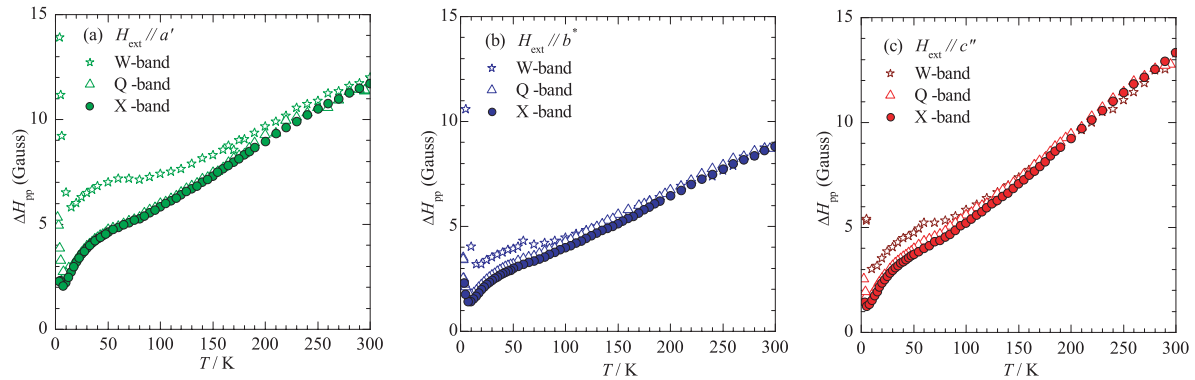

Fig. 6. Temperature and frequency dependence of the ESR linewidth of γ-(BEDT-TTF)$_2$PF$_6$.

noise ratio. In contrast to the ζ-salt, the ESR signal intensity of the γ-salt reached toward a finite value at the lowest temperature.

Here, we discuss the difference between the ζ-salt and γ-salt in the aspect of magnetic dimensionality. The exchange interaction, J, was roughly about $\approx$30 K considering the local maximum temperature of χ_p for the both salts. The antiferromagnetic transition temperature, T_N, was about 5 K for the ζ-salt. The estimated $k_B T_N/J$ of the ζ-salt was about 0.2, which is higher than that of a typical one-dimensional antiferromagnet such as Cu benzoate (0.088).[21] Hence, we expect considerable two- (or three-) dimensional interaction for the ζ-salt. On the other hand, no long-range order was observed down to 4 K for the γ-salt. The absence of magnetic long-range ordering suggests that the γ-salt has highly one-dimensionality and/or quantum fluctuation.

In order to determine the magnetic dimensionality of the ζ-salt and the γ-salt, we measured the detailed temperature dependence of the ESR linewidth ΔH. The ESR linewidth basically contains information about the spin–lattice and spin–spin relaxation times. Figures 5 and 6 shows ΔH for the ζ-salt and γ-salt obtained by X-, Q-, and W-bands ESR as a function of temperature, respectively.

As shown in Fig. 5, the ΔH of the ζ-salt was constant in the temperature range from 25 to 296 K, which is consistent with the expected results for the paramagnetic phase of conventional spin systems with antiferromagnetic interactions. No obvious microwave frequency dependence of ΔH was observed in this temperature region for the ζ-salt, indicating that the exchange coupling correlation rate ($1/\tau$–$J/\hbar$) is much higher than the Larmor (microwave) frequencies (f_L). The increase in ΔH below 30 K is explained by critical slowing down phenomena observed for the long-range magnetic order. In the region of critical slowing down, ΔH showed slight microwave frequency dependence. Since the deviation of the ΔH due to the frequency dependence is comparable to the experimental error, we cannot make a clear explanation at present. However, it seems likely that the ΔH increases with an increase in the frequency in all directions. Roughly speaking, as the system approaches to the antiferromagnetic transition temperature (T_N), the exchange coupling correlation rate, $1/\tau$, rapidly decreases and goes to zero toward T_N. In other words, the spectral density shifts to lower the frequency region as the temperature decreases. On the other hand, the electron spin relaxation rate shows a maximum at the temperature where $f_L = 1/\tau$. In general, the exchange coupling correlation rate is much higher than Larmor frequencies. Hence, the linewidth maximum temperature is very close to T_N as for the three-dimensional magnet. The electron spin relaxation rate seems likely to increase as the Larmor frequency increases. It is also noted that precursor temperature region is much narrower than that of the γ-salt, and that seems to be a typical behavior of a conventional antiferromagnet. These observations indicate that the ζ-salt is basically two-dimensional magnet with considerable three-dimensional interaction.

The frequency and temperature dependence of the ΔH of the γ-salt are also shown in Fig. 6. The situation is rather complicated in the case of the γ-salt, as follows. One particular

feature of the γ-salt is that the ΔH decreased as the temperature decreased down to 10 K for all directions. In the case of the localized spin system, the origin of the ESR linewidth is basically due to internal dipolar field and exchange narrowing effect. These two physical parameters are temperature independent for conventional magnets. However, in the case of one-dimensional $S = 1/2$ antiferromagnet, electron-spin relaxation by exchange interaction is not effective, and curious temperature dependence of the ΔH are frequently observed.[22–24] Although extensive theoretical studies have been carried out on one-dimensional antiferromagnets, so far, quantitative analyses of the ESR linewidth are not easy. Recently, Oshikawa and Affleck have developed low-temperature ESR theory for half-integer spin antiferromagnetic chains using field theory method.[25] According to their theory, an exchange anisotropy gives ΔH linear dependence on temperature and independence on magnetic field over an intermediated temperature range. The temperature dependence of the ΔH of the γ-salt is consistent with the prediction from their theory. We cannot explain the origin of the slight hump in the ΔH observed at around 30 K, which is close to J. However, it is noted that a similar hump has also been observed at around $T/J \approx 1$ in a one-dimensional system, α'-NaV_2O_5.[26]

The decrease in ΔH with a decrease in temperature is commonly observed for X-, Q-, and W-bands down to 10 K. No obvious difference was observed between the results of the X- and Q-bands ESR measurement over the entire temperature range. On the other hand, a significant increase in ΔH was observed below 150 K in the case of the W-band. The broadening was pronounced along the a'-axis, which is the direction of structural one-dimensional chain. However, the independence on the magnetic field of ΔH is expected from the Oshikawa–Affleck theory over an intermediated temperature range if we assume only exchange anisotropy. Possible explanations are as follows. (1) If the microwave frequency is comparable with the exchange coupling correlation rate, $1/\tau$, the ESR linewidth could be broadened in order to break down the averaged g-value. However, the lineshape does not change below 150 K. Moreover, no systematic broadening of the ΔH was observed in the Q-band. Hence, this possibility can be ruled out. (2) Another possible explanation is a transverse staggered field effect. We do not have any evidence for the presence of a Dzyaloshinsky–Moriya interaction, since antiferromagnetic transition was not observed down to the lowest temperature for the γ-salt. However, there are two crystallographically independent BEDT-TTF dimers ($S = 1/2$) in the unit cell, as seen in the next session. These dimers stack to form a one-dimensional column, in which BEDT-TTF dimers are twisted, indicating a staggered g-tensor system. Moreover, there is a crystallographical center of symmetry at the midpoint of the one of dimers. Hence, each $S = 1/2$ spin is not connected by the inversion symmetry. Possible transverse staggered field effect for the ESR parameters have been discussed for the several one-dimensional $S = 1/2$ system.[18,27] In these systems, a transverse staggered field effect gives a B/T^2 component for the linewidth and B/T^3 term for the resonance filed according to the Oshikawa–Affleck theory. As a result, the ΔH shows a local minimum and frequency dependence at low temperatures. For example, $Cu(C_6H_5COO)_2 \cdot 3H_2O$, of which $J \cong 8.6$ K, shows a local minimum of the ΔH at around 5 K, and frequency dependence of the ΔH has been observed below 20 K as for 9.4–48 GHz measurements.[18,21] In the case of the $BaCu_2(Si_{1-x}Ge_x)_2O_7$ ($J \cong 470$ K), the local minimum of the ΔH at around 10–100 K, and frequency dependent ΔH was observed below in the whole temperature region ($T < 300$ K) for 9–300 GHz.[28] Although we cannot perform quantitative analysis at present, it should be noted that the anomalous behavior of the γ-salt ($J \cong 25$ K) was observed in the intermediated temperature region between the two one-dimensional antiferromagnets mentioned above.

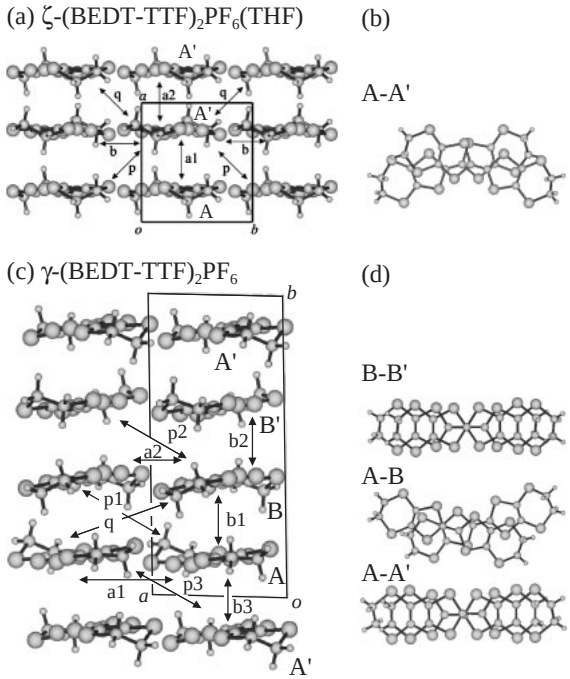

Fig. 7. Crystal structure of ζ-$(BEDT\text{-}TTF)_2PF_6(THF)$ and γ-$(BEDT\text{-}TTF)_2PF_6$. (a) The alignment of BEDT-TTF molecules viewed along the molecular long axis of ζ-salt. (b) Overlapping mode of stacking BEDT-TTF of the ζ-salt projected along the stacking axis. (c) The BEDT-TTF alignment of the γ-salt. (d) BEDT-TTF overlapping mode of the γ-salt projected along stacking axis.

Overlap Integrals and Energy Band Structure with Crystal Structure. In order to discuss the magnetic dimensionality in the aspect of crystallographical point of view, we calculated the overlap integrals and energy bands.

The crystal structure perpendicular to the BEDT-TTF layer and calculated overlap integrals are shown in Fig. 7 and Tables 1, 2, respectively. The overlap integrals are comparable to those reported in Ref. 1 for ζ-salt and δ'-$(BEDT\text{-}TTF)_2BrC_2H_4(OH)_2$. The δ'-salt structurally resembles the γ-salt. Using the estimated transfer integrals from $t = ES$, the energy bands were calculated. Since the ζ- and γ-salts are insulators below room temperature, there are no actual Fermi surfaces. However, in order to understand the electronic dimensionality we estimated the virtual Fermi surfaces for these salts, neglecting the correlation gap that originates from a strong dimerization effect. The band structure and Fermi surfaces obtained are shown in Figs. 8 and 9.

Table 1. Calculated Overlap Integrals of ζ-(BEDT-TTF)$_2$-PF$_6$(THF)

Overlap	S ($\times 10^{-3}$)
a1	9.2
a2	8.4
b	9.9
p	2.3
q	1.8

Table 2. Calculated Overlap Integrals of γ-(BEDT-TTF)$_2$-PF$_6$

Overlap	S ($\times 10^{-3}$)
b1	3.5
b2	22.9
b3	23.9
a1	3.5
a2	1.1
p1	0.1
p2	4.8
p3	7.4
q	2.8

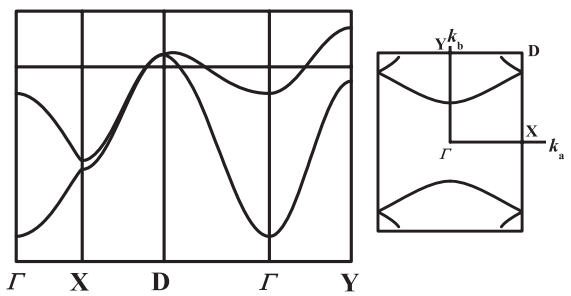

Fig. 8. Energy band structure and Fermi surface of ζ-(BEDT-TTF)$_2$PF$_6$(THF).

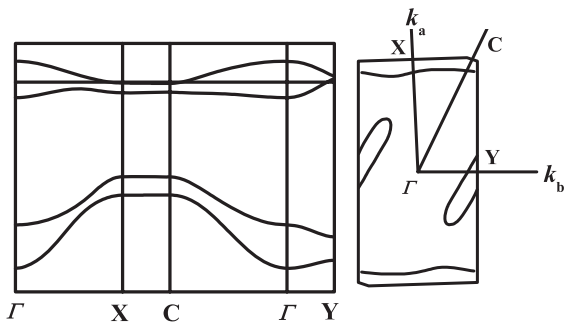

Fig. 9. Energy band structure and Fermi surface of γ-(BEDT-TTF)$_2$PF$_6$.

The crystal structure and calculated value of the overlap integrals of the ζ-salt are shown in Fig. 7a and Table 1, respectively. BEDT-TTF molecules stack along the a-axis with twisting as shown in Fig. 7b. In the case of a ζ-salt, the short S–S contact (3.44 Å) is observed along the transverse direction. As for along the stacking direction, the shortest inter-molecular S–S distance is 3.69 Å. The absolute values of the overlap integrals a1 and a2 show no obvious difference, indicating that there is no strong dimerization. The transverse interaction

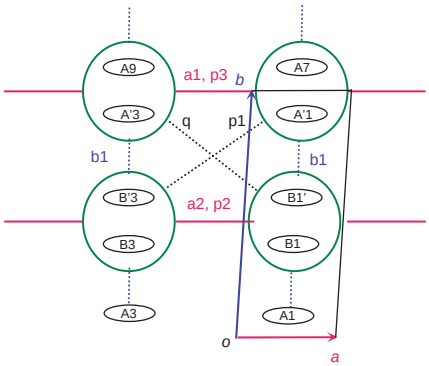

Fig. 10. Schematic viewgraph standing on BEDT-TTF dimer as a unit for the γ-(BEDT-TTF)$_2$PF$_6$. A green circle indicates a dimer, which consists the one-dimensional chain along a-axis (red solid line) with interchain interaction such as b1 overlap.

b is also close to a1 and a2. Therefore, the electronic structure of the ζ-salt can be expressed as two-dimensional. As seen in Fig. 8, the band calculation actually indicates the existence of the closed Fermi surface for the ζ-salt. If we remain the fact that the ζ-salt undergoes an antiferromagnetic transition at 5 K, it is likely that there is considerable two- (and three-) dimensional exchange interactions in this system. Standing on this scenario, the conclusion deduced from the multi-frequency ESR measurements as discussed in the previous session is consistent with the band calculation.

The crystal structure of the γ-salt is shown in Fig. 7c. The space group of the γ-salt is $P\bar{1}$ and $Z = 2$ and contains four BEDT-TTF molecules (A, A′, B, and B′). The BEDT-TTF molecules stack along the b^*-axis, repeating the two stacking manners with the parallel and twisting molecular long axis. Here, we defined the averaged molecular short- and long-axes (principal axes of the $\boldsymbol{g}$-tensor) as a'- and c''-axes, respectively. A and B are related to the A′ and B′ by an inversion center, respectively. The stacking manners of the A–A′, A–B, and B–B″ are shown in Fig. 7d. Slipped stacking is observed in A–A′ and B–B′. On the other hand, the A–B stacking is twisted. The S–S distance between two BEDT-TTF molecules along the a'-axis (side-by-side direction) is 3.42 Å, which is shorter than the van der Waals radii (3.6 Å). On the other hand, the S–S short contact is not observed along the b^*-axis (molecular stacking direction). The shortest inter-molecular S–S distance between the A–A′, A–B, and B–B″ is 3.76, 3.72, and 3.67 Å, respectively.

The overlap integrals b2 and b3 are significantly larger than b1 shown in Table 2. In conparison to the case of the ζ-salt, the BEDT-TTF molecules might be strongly dimerized through the interactions b2 and b3 for the γ-salt, although a short S–S contact also does not exist along the b^*-axis and the dimers form the one-dimensional chain along the a'-axis. Figure 10 shows a schematic viewgraph standing on the BEDT-TTF dimer as a unit for the γ-salt. We can find significant inter-dimer interactions through both a1 and p3 in the transverse direction, suggesting possible BEDT-TTF dimer chains along the a'-axis. The sum of the inter-chain interactions through b1, p1, and q are much less than the total inter-chain interaction. Hence, we can consider the γ-salt as an $S =$

1/2 quasi-one-dimensional Heisenberg spin system. If we ignore electric correlation effect (actually this salt is an insulator), the virtual Fermi surface is shown in Fig. 9. There are clear open one-dimensional Fermi sheets for the γ-salt. Although coexistence of a small two-dimensional surface apparently reflects finite interchain interactions, the area of the Fermi surface is tiny. These results support that the γ-salt has the magnetic one-dimensionality which was determined from the multi-frequency ESR measurements.

Conclusion

We investigated the magnetic properties for ζ-(BEDT-TTF)$_2$PF$_6$(THF) and γ-(BEDT-TTF)$_2$PF$_6$ by magnetic measurements, multi-frequency ESR spectroscopy and theoretical calculation of energy bands. No apparent difference between these salts was observed from the macroscopic magnetic susceptibility results. However, obvious differences found in the results of ESR measurements, and we tried to explain the experimental results in the framework of magnetic dimensionality: γ-(BEDT-TTF)$_2$PF$_6$ behaved as a quasi-one-dimensional antiferromagnet without long range ordering down to 4 K, whereas ζ-(BEDT-TTF)$_2$PF$_6$(THF) behaved as a classical three-dimensional antiferromagnet with antiferromagnetic long range ordering at 5 K. These considerations were also supported by the theoretical calculation of the energy bands. In this paper, we pointed out the importance the microscopic multi-frequency magnetic resonance investigation to discuss the exact magnetic properties of low-dimensional electronic systems.

The authors thank M. Sakai (IMS) for the help in ESR. This work was partly supported by a Grant-in-Aid for Scientific Research on Priority Areas of Molecular Conductors (No. 15073223) from the Ministry of Education, Culture, Sports, Science and Technology, Japan.

References

1 T. Mori, *Bull. Chem. Soc. Jpn.* **1999**, *72*, 2011.
2 T. Mori, *Bull. Chem. Soc. Jpn.* **1998**, *71*, 2509.
3 T. Mori, H. Mori, S. Tanaka, *Bull. Chem. Soc. Jpn.* **1999**, *72*, 179.
4 G. K. R. Senadeera, T. Kawamoto, T. Mori, J. Yamaura, T. Enoki, *J. Phys. Soc. Jpn.* **1998**, *67*, 4193.
5 Y. Ding, H. Tajima, *Phys. Rev. B* **2004**, *69*, 115121.
6 X. Bu, I. Cisarova, P. Coppens, *Acta Crystallogr., Sect. C* **1992**, *48*, 1563.
7 M. A. Beno, M. A. Firestone, P. C. W. Leung, L. M. Sowa, H. H. Wang, J. M. Williams, M.-H. Whangbo, *Solid State Commun.* **1986**, *57*, 735.
8 X. Bu, I. Cisaroba, P. Coppens, B. Lederle, M. J. Naughton, *Acta Crystallogr., Sect. C* **1992**, *48*, 516.
9 T. Mallah, C. Hollis, S. Bott, M. Kurmoo, P. Day, M. Allan, R. H. Friend, *Dalton Trans.* **1990**, 859.
10 H. Yu, B. Zhang, D. Zhu, *J. Mater. Chem.* **1998**, *8*, 77.
11 K. Maeda, T. Hara, T. Nakamura, *Synth. Met.* **2005**, *152*, 453. In this paper, γ-(BEDT-TTF)$_2$PF$_6$ is expressed as α-(BEDT-TTF)$_2$PF$_6$. This material was characterized as γ-(BEDT-TTF)$_2$PF$_6$ by the subsequent X-ray crystal structure analysis.
12 T. Mori, A. Kobayashi, Y. Sasaki, H. Kobayashi, G. Saito, H. Inokuchi, *Bull. Chem. Soc. Jpn.* **1984**, *57*, 627.
13 T. Mori, M. Katsuhara, *J. Phys. Soc. Jpn.* **2002**, *71*, 826.
14 W. E. Hatfield, R. R. Weller, J. W. Hall, *Inorg. Chem.* **1980**, *19*, 3825.
15 J. C. Bonner, M. E. Fisher, *Phys. Rev.* **1964**, *135*, A640.
16 T. Nakamura, W. Minagawa, R. Kinami, T. Takahashi, *J. Phys. Soc. Jpn.* **2000**, *69*, 504.
17 K. Nagata, Y. Tazuke, *J. Phys. Soc. Jpn.* **1972**, *32*, 337.
18 H. Ohta, K. Kirita, T. Kunimoto, S. Okubo, Y. Hosokoshi, K. Katoh, K. Inoue, A. Ogasahara, S. Miyashita, *J. Phys. Soc. Jpn.* **2002**, *71*, 2640.
19 S. Miyashita, T. Yoshino, A. Ogasahara, *J. Phys. Soc. Jpn.* **1999**, *68*, 655.
20 T. Nakamura, *J. Phys. Soc. Jpn.* **2000**, *69*, 4026.
21 K. Oshima, K. Okuda, M. Date, *J. Phys. Soc. Jpn.* **1978**, *44*, 757.
22 K. Okuda, H. Hata, M. Date, *J. Phys. Soc. Jpn.* **1972**, *33*, 1574.
23 Y. Ajiro, S. Matsukawa, T. Yamada, T. Haseda, *J. Phys. Soc. Jpn.* **1975**, *39*, 259.
24 N. Yoneyama, A. Miyazaki, T. Enoki, G. Saito, *Bull. Chem. Soc. Jpn.* **1999**, *72*, 639.
25 M. Oshikawa, I. Affleck, *Phys. Rev. B* **2002**, *65*, 134410.
26 I. Yamada, H. Manaka, H. Sawa, M. Nishi, M. Isobe, Y. Ueda, *J. Phys. Soc. Jpn.* **1998**, *67*, 4269.
27 M. Oshikawa, I. Affleck, *Phys. Rev. Lett.* **1999**, *82*, 5136.
28 S. Okubo, D. Fukuoka, M. Kimata, H. Ohta, Y. Inagaki, T. Kumimoto, K. Koyama, M. Motokawa, Z. Hiroi, *J. Phys. Soc. Jpn.* **2005**, *74*, Suppl. 80.